J|A|C|S
ARTICLES

Catalytic Mechanism of a Heme and Tyrosyl Radical-Containing Fatty Acid α-(Di)oxygenase

Arnab Mukherjee, Alfredo M. Angeles-Boza, Gregory S. Huff, and Justine P. Roth*

Department of Chemistry, Johns Hopkins University, 3400 North Charles Street, Baltimore, Maryland 21218, United States

Received May 14, 2010; E-mail: jproth@jhu.edu

Abstract: The steady-state catalytic mechanism of a fatty acid α-(di)oxygenase is examined, revealing that a persistent tyrosyl radical (Tyr379$^\bullet$) effects O_2 insertion into C_α−H bonds of fatty acids. The initiating C_α−H homolysis step is characterized by apparent rate constants and deuterium kinetic isotope effects (KIEs) that increase hyperbolically upon raising the concentration of O_2. These results are consistent with H$^\bullet$ tunneling, transitioning from a reversible to an irreversible regime. The limiting deuterium KIEs increase from ∼30 to 120 as the fatty acid chain is shortened from that of the native substrate. In addition, activation barriers increase in a manner that reflects decreased fatty acid binding affinities. Anaerobic isotope exchange experiments provide compelling evidence that Tyr379$^\bullet$ initiates catalysis by H$^\bullet$ abstraction. C_α−H homolysis is kinetically driven by O_2 trapping of the α-carbon radical and reduction of a putative peroxyl radical intermediate to a 2(*R*)-hydroperoxide product. These findings add to a body of work which establishes large-scale hydrogen tunneling in proteins. This particular example is novel because it involves a protein-derived amino acid radical.

Introduction

There is substantial evidence that amino acid radicals act as cofactors in a number of redox-active metalloenzymes,[1−4] yet detailed mechanistic studies have been somewhat limited.[5] This is particularly true of heme proteins where spectroscopic features of the radical are obscured by the Soret absorption band of the prosthetic group, making it a challenge to evaluate catalytic competence.[6,7] Examination of the kinetics and thermodynamics that characterize amino acid radical-mediated hydrogen atom transfer is needed to characterize this seemingly general strategy in enzyme catalysis.[1−6,8]

Tyrosyl radicals (Tyr$^\bullet$) are particularly widespread, having been spectroscopically observed[9] and/or implicated as interme-

diates in photosystem II,[2,10] ribonucleotide reductase,[11] cytochrome *c* oxidase,[12] and several heme-containing peroxidases[13] as well as dioxygenases.[3,4b,14−16] The fatty acid α-(di)oxygenase from rice (RαO) is the focus of the present study. In RαO, a Tyr$^\bullet$ is produced as a result of oxidizing ferric protoporphyrin IX, Fe^{III}(Por), with H_2O_2. Coordination of H_2O_2 followed by O−O bond heterolysis generates a ferryl π-cation radical, Fe^{IV}=O(Por$^{\bullet+}$), which may react by intraprotein proton-coupled electron transfer,[3] producing Fe^{IV}=O(Por), a protonated base, and Tyr379$^\bullet$ as shown in eq 1.

RαO is a plant-derived pathogen-inducible (di)oxygenase (PIOX).[15−17] Members of this family of heme proteins possess a conserved Tyr and exhibit roughly 30% structural homology

(1) (a) Stubbe, J.; van der Donk, W. A. *Chem. Rev.* **1998**, *98*, 705–762. (b) Pesavento, R. P.; van der Donk, W. A. *Adv. Protein Chem.* **2001**, *58*, 317.
(2) Diner, B. A.; Britt, R. D. *Adv. Photosynth. Respir.* **2005**, *22*, 207–233.
(3) Rouzer, C. A.; Marnett, L. J. *Chem. Rev.* **2003**, *103*, 2239–2304.
(4) Evidence of catalytic tyrosyl radicals in plant-derived heme-containing dioxygenases:(a) Su, C.; Sahlin, M.; Oliw, E. H. *J. Biol. Chem.* **1998**, *273*, 20744–20751. (b) Gupta, A.; Mukherjee, A.; Matsui, K.; Roth, J. P. *J. Am. Chem. Soc.* **2008**, *130*, 11274–11275.
(5) (a) Licht, S.; Gerfen, G. J.; Stubbe, J. *Science* **1996**, *271*, 477–81. (b) Aubert, C.; Vos, M. H.; Mathis, P.; Eker, A. P. M.; Brettel, K. *Nature* **2000**, *405*, 586–590. (c) Mozziconacci, O.; Williams, T. D.; Kerwin, B. A.; Schoneich, C. *J. Phys. Chem. B* **2008**, *112*, 15921–15932.
(6) Tsai, A.-L.; Kulmacz, R. J. *Arch. Biochem. Biophys.* **2010**, *493*, 103–24.
(7) Wu, G.; Rogge, C. E.; Wang, J.-S.; Kulmacz, R. J.; Palmer, G.; Tsai, A.-L. *Biochemistry* **2007**, *46*, 534–542.
(8) Himo, F.; Siegbahn, P. E. M. *Chem. Rev.* **2003**, *103*, 2421–2456.
(9) (a) Svistunenko, D. A.; Jones, G. A. *Phys. Chem. Chem. Phys.* **2009**, *11*, 6600–6613. (b) Svistunenko, D. *Biochim. Biophys. Acta* **2005**, *1707*, 127–155.

(10) (a) Jenson, D. L.; Barry, B. A. *J. Am. Chem. Soc.* **2009**, *131*, 10567–10573. (b) Kuehne, H.; Brudvig, G. W. *J. Phys. Chem. B* **2002**, *106*, 8189–8196.
(11) Stubbe, J. *Curr. Opin. Chem. Biol.* **2003**, *7*, 183–188.
(12) (a) Siletsky, S. A.; Han, D.; Brand, S.; Morgan, J. E.; Fabian, M.; Geren, L.; Millett, F.; Durham, B.; Konstantinov, A. A.; Gennis, R. B. *Biochim. Biophys. Acta, Bioenerg.* **2006**, *1757*, 1122–1132. (b) Bu, Y.; Cukier, R. I. *J. Phys. Chem. B* **2005**, *109*, 22013–22026. (c) Proshlyakov, D. A.; Pressler, M. A.; Babcock, G. T. *Proc. Natl. Acad. Sci. U.S.A.* **1998**, *95*, 8020–8025.
(13) (a) Furtmueller, P. G.; Zederbauer, M.; Jantschko, W.; Helm, J.; Bogner, M.; Jakopitsch, C.; Obinger, C. *Arch. Biochem. Biophys.* **2006**, *445*, 199–213. (b) Fielding, A. J.; Singh, R.; Boscolo, B.; Loewen, P. C.; Ghibaudi, E. M.; Ivancich, A. *Biochemistry* **2008**, *47*, 9781–9792. (c) Divi, R. L.; Doerge, D. R. *Biochemistry* **1994**, *33*, 9668–74. (d) Ehrenshaft, M.; Mason, R. P. *Free Radical Biol. Med.* **2006**, *41*, 422–30.
(14) Kulmacz, R. J.; van der Donk, W. A.; Tsai, A.-L. *Prog. Lipid Res.* **2003**, *42*, 377–404.
(15) Hamberg, M.; Ponce de Leon, I.; Sanz, A.; Castresana, C. *Prostaglandins Other Lipid Mediators* **2002**, *68/69*, 363–374.
(16) Koeduka, T.; Matsui, K.; Akakabe, Y.; Kajiwara, T. *J. Biol. Chem.* **2002**, *277*, 22648–22655.
(17) Smith, W. L.; DeWitt, D. L.; Garavito, R. M. *Annu. Rev. Biochem.* **2000**, *69*, 145–182.

$$+ H_2O_2 \quad (1)$$
$$- H_2O$$
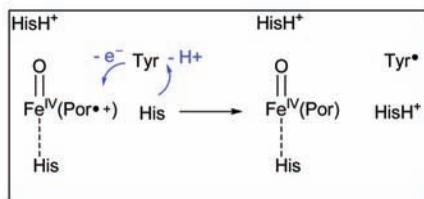
to the mammalian prostaglandin H_2 synthases, also known as the cyclooxygenases (COX-1 and COX-2).[16] The cyclooxygenases catalyze the first dedicated step in prostaglandin biosynthesis from arachidonic acid, thereby controlling the formation of prostanoids that effect a range of physiological and pathophysiological functions; inflammation is perhaps the most recognized.[17–19] Analogously, the PIOX family of proteins produces oxylipoxins that participate in cell signaling, wound healing, and the plant's immune response.[15]

Studies employing site-directed mutagenesis and electron paramagnetic resonance (EPR) spectroscopy have provided evidence that the Tyr379• is required for catalytic functioning of RαO.[4b,16,20] The mutant Tyr379Phe-RαO is devoid of fatty acid dioxygenase activity as well as the persistent EPR signal found in samples of the wild-type (wt) RαO at ambient temperature. The stability of the $Fe^{IV}=O(Por^{\bullet+})$ is enhanced in Tyr379Phe-RαO relative to wt-RαO and other heme proteins.[21] The quantitative formation of this species can be observed, followed by its slow decay to $Fe^{IV}=O(Por)$ and eventually back to $Fe^{III}(Por)$ over several seconds.

RαO provides an ideal model system for understanding COX and related enzymes that catalyze reactions using amino acid radicals.[1–8] Though mutagenesis studies have implicated the conserved Tyr• in dioxygenase activity,[4b,22,23] questions remain as to how the radical is formed and endowed with the thermodynamic and kinetic propensity to oxidize fatty acids. RαO reacts with its substrates specifically at the acidic $C_\alpha-H$ bond adjacent to the carboxylate. Detailed studies of RαO catalysis have been facilitated by the large quantities of pure protein that can be isolated, together with the protein's stability with respect to oxidative damage.

RαO is recombinantly expressed in *Escherichia coli*, largely in the form of the $Fe^{III}(Por)$-containing holoprotein.[16,24,25] Though a crystal structure is not yet available,[26] homology models[4b,17] featuring a conserved tyrosine, ∼6 Å from the

metalloporphyrin edge, have been constructed on the basis of a COX-1 structure.[27] Given the inherent uncertainty of homology models, it is unclear whether a nearby histidine, His311, is close enough to influence formation of Tyr379• through hydrogen bonding[28] or whether it is strategically placed, remote from the catalytic radical, where it can anchor the carboxylate tail of the fatty acid.[17,29]

Fatty acid oxidation by RαO produces 2(*R*)-hydroperoxide compounds (eq 2).[16] These species are only moderately stable at low temperatures and undergo spontaneous (non-enzymatic) decarboxylation to form C_{n-1} aldehydes, as depicted in eq 2. Although the aldehyde is the only detectable product after workup,[4b,16] a small fraction of the initially formed 2(*R*)-hydroperoxide is likely to react with Fe^{III}-RαO by $2e^-$ oxidation. Such a reaction, where the product activates the enzyme, accounts for the ability of RαO to catalyze fatty acid oxidation in the absence of added radical initiators, such as H_2O_2.

$$(2)$$
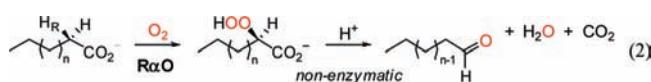
In this paper we describe the steady-state catalytic mechanism of RαO revealed by studies of initial rates, substrate deuterium kinetic isotope effects (KIEs), and solvent isotope exchange. Saturated fatty acids (FAs) of variable chain length, hexadecanoic acid (16:0), dodecanoic acid (12:0), and decanoic acid (10:0), are used to establish the kinetic mechanism as well as the limiting rate constants and KIEs that reflect homolytic cleavage of the $C_\alpha-H$ bond. The molecular oxygen concentration is shown to affect the reversibility of initial H• abstraction from the fatty acid. Analysis of the rate-limiting step at low O_2 concentrations, where $C_\alpha-H$ homolysis is reversible, is the subject of a separate study.[30]

Under conditions of O_2 saturation, $C_\alpha-H$ homolysis is characterized by large deuterium KIEs which range from ∼30 to 120. These effects are consistent with extensive nuclear tunneling in the turnover-controlling step, as proposed in preliminary studies with the native substrate, 16:0.[4b] Here it is demonstrated that the deuterium KIEs become larger upon shortening the fatty acid chain. Inflation of the deuterium KIE is accompanied by a marked decrease in $k_{cat}/K_M(FA)$, by 2 orders of magnitude, but little variation in k_{cat}. Thus, while nuclear tunneling is an inherent feature of H• abstraction from C−H bonds, it is not obvious to what extent the probability of this reaction is influenced by RαO,[31] nor is it evident how the enzyme controls O_2 addition to the incipient α-carbon radical,

(18) Choi, S.-H.; Aid, S.; Bosetti, F. *Trends Pharmacol. Sci.* **2009**, *30*, 174–181.

(19) Marnett, L. J. *Annu. Rev. Pharmacol. Toxicol.* **2009**, *49*, 265–290.

(20) Koszelak-Rosenblum, M.; Krol, A. C.; Simmons, D. M.; Goulah, C. C.; Wroblewski, L.; Malkowski, M. G. *J. Biol. Chem.* **2008**, *283*, 24962–24971.

(21) Dunford, H. B. *Heme Peroxidases*; Wiley: New York, 1999.

(22) (a) Karthein, R.; Dietz, R.; Nastainczyk, W.; Ruf, H. H. *Eur. J. Biochem.* **1988**, *171*, 313–20. (b) Dietz, R.; Nastainczyk, W.; Ruf, H. H. *Eur. J. Biochem.* **1988**, *171*, 321–8.

(23) Mukherjee, A.; Brinkley, D. W.; Chang, K.-M.; Roth, J. P. *Biochemistry* **2007**, *46*, 3975–3989.

(24) A homologue from *Arabidopsis thaliana* has also been described: (a) Liu, W.; Rogge, C. E.; Bambai, B.; Palmer, G.; Tsai, A.-L.; Kulmacz, R. J. *J. Biol. Chem.* **2004**, *279*, 29805–29815. (b) Liu, W.; Wang, L.-H.; Fabian, P.; Hayashi, Y.; McGinley, C. M.; van der Donk, W. A.; Kulmacz, R. J. *Plant Physiol. Biochem.* **2006**, *44*, 284–293.

(25) Typical R_z values are ≥0.4 for the isolated holoproteins. The addition of neither hemin nor hematin results in a discernible increase in specific activity.

(26) Lloyd, T.; Krol, A.; Campanaro, D.; Malkowski, M. *Acta Crystallogr., Sect. F* **2006**, *F62*, 365–367.

(27) Malkowski, M. G.; Ginell, S. L.; Smith, W. L.; Garavito, R. M. *Science* **2000**, *289*, 1933–1937.

(28) Wilson, J. C.; Wu, G.; Tsai, A.-L.; Gerfen, G. J. *J. Am. Chem. Soc.* **2005**, *127*, 1618–1619.

(29) Bhattacharyya, D. K.; Lecomte, M.; Rieke, C. J.; Garavito, R. M.; Smith, W. L. *J. Biol. Chem.* **1996**, *271*, 2179–84.

(30) Huff, G. S.; Doncheva, I. S.; Angeles-Boza, A. M.; Mukherjee, A.; Brinkley, D. W. Cramer, C. J.; Roth, J. P. Manuscript in preparation.

(31) (a) Benkovic, S. J.; Hammes-Schiffer, S. *Science* **2006**, *312*, 208–209. (b) Hammes-Schiffer, S.; Benkovic, S. J. *Annu. Rev. Biochem.* **2006**, *75*, 519–541.

resulting in the formation of the 2(R)-hydroperoxide product with high regio- and stereochemical fidelity.

Experimental Section

General Procedures. Chemical reagents were obtained from Sigma-Aldrich in the highest purity available (>98%) and used without further purification unless noted. Deuterium-labeled materials were obtained from Cambridge Isotope Laboratories and used as received. Hydrogen peroxide (30%) was obtained from Fisher and its concentration determined using the well-known optical extinction coefficient $\varepsilon_{240\,nm} = 43.6$ M^{-1} cm^{-1}. Substrate-containing solutions were prepared just prior to use by dilution of the fatty acids dissolved in ethanol into the reaction buffer and stirring under an atmosphere of air, He/O$_2$ or N$_2$/O$_2$.

Electronic absorption measurements were performed using an Agilent 8453 diode array or OLIS stopped-flow RSM 1000 spectrophotometer. EPR spectra were recorded on a Bruker X-band (9.395 GHz) spectrometer as previously described.[4b] The persistent Tyr379$^\bullet$ was further probed by power saturation experiments at 15 K. The power was varied from 20.1 μW to 20.1 mW while the modulation amplitude was maintained at 10 G. $P_{1/2}$, corresponding to the power at half-saturation, was derived from the standard equation: $\log(S/P^{1/2}) = -(b/2) \log(P_{1/2} + P) + (b/2) \log(P_{1/2}) + \log K$, where P is the power, S is the peak to trough amplitude of the EPR signal, b is the inhomogeneity parameter ($\sim$1), and K is a floating parameter.

A Clark-type O$_2$ electrode[32] (Yellow Springs Inc.) was used to record changes in the concentration of O$_2$ with time. Readings from the voltmeter were transmitted to a PC workstation with a 1 s sampling time. The electrode probe, equipped with a 10 μL injection port, was fitted inside a transparent water-jacketed reaction chamber, connected to a temperature-controlled recirculating bath (VWR 116-0S), and used atop a magnetic stirrer.

Density functional theory (DFT) calculations were performed using Gaussian03.[33] A calibrated method,[30] employing the modified Perdew−Wang (mPWPW91) functional and the following basis set 6-311G* (O), 6-31G (C), and STO-3G (H), was used to obtain energy-minimized structures which were subject to vibrational frequency analyses.[34] Calculations of deuterium equilibrium isotope effects were performed by analyzing isotopic zero-point energy differences associated with the symmetric C−H(D) and O−H(D) stretches of butanoate and 4-hydroxyphenylacetate, which serve as models for the longer chain fatty acids and reduced tyrosine.[35] It was confirmed that no other vibrational frequencies changed significantly upon this isotopic substitution.

Protein Preparation, Characterization, and Quantification. The genes encoding wt-RαO and Tyr379Phe-RαO were sequenced[36] and overexpressed to obtain N-terminal His-tagged proteins.[4b,16] Affinity chromatography afforded proteins of ≥98% purity as indicated by polyacrylamide gel electrophoresis and amino acid sequencing (Texas A&M University Protein Chemistry Facility). A slight modification of the published procedure[16] involved dialysis of the concentrated protein against 50 mM sodium phosphate buffer (pH 7.2) to remove most of the NaCl and Nonidet P-40 or Nonidet P-40 substitute used during protein isolation.

Removal of these additives allowed for control experiments that tested the possibility of kinetic artifacts arising from the presence of salt or detergent.[37]

The concentrations of wt-RαO and Tyr379Phe-RαO were determined by UV−vis spectrophotometry using the molar extinction coefficients of the Fe^{III}(Por) Soret absorption band. The pyridine hemochrome assay[38] was performed under oxidizing and reducing conditions to obtain average values of $\varepsilon_{412\,nm} = 123\,000$ M^{-1} cm^{-1} for wt-RαO and $\varepsilon_{410\,nm} = 157\,000$ M^{-1}cm^{-1} for the Tyr379Phe mutant. The wt enzyme's specific activity, optimized by addition of H$_2$O$_2$,[37] correlated to the concentration of Fe^{III}(Por) determined spectrophotometrically. This relationship, which held for multiple preparations of the wt protein, was used to develop a standard assay for the determination of the active enzyme concentration. Under no conditions was fatty acid dioxygenase activity detectable in the Tyr379Phe mutant.

A 1:1 relationship between Fe^{III}(Por) and active wt-RαO containing Tyr379$^\bullet$ was assumed in the steady-state kinetic analysis. The formation of the radical appears to require two-electron oxidation of the Fe^{III} prosthetic group to the Fe^{IV}=O(Por$^{\bullet+}$) state (cf. eq 1). Only one oxidizing equivalent can be accounted for, however, by formation of Tyr379$^\bullet$. Prior to treatment of wt-RαO with H$_2$O$_2$, a trace amount of this radical with an EPR signature at $g = 2.0054$, is detectable at 295 K.[4b] Following the addition of 10−100 equiv of H$_2$O$_2$, the EPR signal intensity increases as does the enzyme's fatty acid dioxygenase activity.[4b,37]

EPR spectroscopy, at ambient and at liquid He temperatures, has been used to characterize the species formed upon manually mixing H$_2$O$_2$ with wt- and Tyr379Phe-RαO.[4b,37] In experiments with the wt protein, the yield of the persistent radical at $g = 2.0054$ is typically 25−30% on the basis of the concentration of Fe^{III}(Por) bound to the holoprotein. No EPR signal is detectable when the Tyr379Phe-RαO is treated in an identical manner; however, the mutant does undergo the expected two-electron oxidation by H$_2$O$_2$. A stabilized Fe^{IV}=O(Por$^{\bullet+}$) is formed and then decays to Fe^{IV}=O(Por) before returning to Fe^{III}(Por) after several hundred seconds at 295 K.[4b] Despite the marked differences in stability associated with the ferryl states in the two proteins, wt-RαO and Tyr379Phe-RαO exhibit comparable catalase-like activities; i.e., the H$_2$O$_2$ disproportionation reactions progress quantitatively, producing 1 equiv of O$_2$ and H$_2$O for every 2 equiv of H$_2$O$_2$ consumed.[37]

Steady-State Kinetics. Initial rates were recorded at 295 K and pH 7.2 in solutions containing 50 mM sodium phosphate ($\mu = 0.1$ M) unless noted otherwise. Though wt-RαO is able to catalyze fatty acid oxidation in the absence of added H$_2$O$_2$, initial rates can be 2−3 times less than the maximum for the slower substrates 12:0 and 10:0.[37] In contrast, preincubation with H$_2$O$_2$ has a smaller effect upon the initial rate of 16:0 oxidation. In most experiments, the enzyme was pretreated with H$_2$O$_2$ (10−100 equiv) to optimize the dioxygenase activity.[37] In other instances, active enzyme concentrations were determined by the standard assay, where $V/[E]_t = 9.0$ s^{-1} for air-saturated solutions containing 270 μM O$_2$ and 100 μM 16:0 at 295 K.

Due to the importance of kinetic trends, a number of control experiments were undertaken to probe for artifacts that could manifest as inhibition or systematic changes in enzyme activity. Prior to each initial rate determination, a background "drift" rate of the O$_2$ electrode was recorded and used to correct the experimentally observed rate when necessary. In experiments with H$_2$O$_2$, a short time was allotted so that O$_2$ evolution due to RαO's catalase-like activity had ceased prior to initiation of the dioxygenase reaction by addition of the fatty acid. In other experiments, which were initiated by the addition of H$_2$O$_2$ pre-treated enzyme, the same rate was obtained. It was regularly verified that O$_2$ consumption rates varied in direct proportion to the wt-RαO concentration. In

(32) Corrections for "dampening effects" were deemed unnecessary: Tsai, A.-L.; Wu, G.; Kulmacz, R. J. *Biochemistry* **1997**, *36*, 13085–13094. The concentrations of O$_2$ determined using the O$_2$ electrode corresponded closely to the amount of aldehyde product formed as indicated by GC−MS as well as the determination of CO$_2$ by manometry.

(33) Frisch, M. J.; et al. *Gaussian 03W*, revision C.02; Gaussian, Inc.: Pittsburgh, PA, 2003. The complete citation appears in the Supporting Information.

(34) Cramer, C. J. *Essentials of Computational Chemistry*, 2nd ed.; Wiley: New York, 2004.

(35) Melander, L.; Saunders, W. H., Jr. *Reaction Rates of Isotopic Molecules*, 2nd ed.; Wiley: New York, 1980.

(36) Sequencing results are provided in the Supporting Information of ref 4b.

(37) See the Supporting Information for details.

(38) Berry, E. A.; Trumptower, B. L. *Anal. Biochem.* **1987**, *161*, 1–15.

addition, the introduction of NaCl ($\leq$30 mM) and detergents such as Nonidet P-40 or Nonidet P-40 substitute ($\leq$0.02%) was found to have no effect on the initial rates.[37]

All kinetic data were analyzed using OLIS Globalworks or Kaleidagraph 4.0 (Synergy Software). Accordingly, all rate constants are reported with $\pm$2 standard errors. The apparent turnover rate constant ($^{ap}k_{cat}$) and the apparent Michaelis constant ($^{ap}K_M$) were routinely obtained by nonlinear curve fitting of initial rate data to the Michaelis–Menten expression. The limiting steady-state kinetic parameters k_{cat} and k_{cat}/K_M were derived from the hyperbolic dependences of $^{ap}k_{cat}$ and $^{ap}k_{cat}/K_M$ upon increasing the concentration of the corresponding cosubstrate.

Deuterium Kinetic Isotope Effects. KIEs were determined for the reactions of deuterium-labeled and unlabeled fatty acids under competitive as well as noncompetitive conditions. As previously described,[4b,39,40] competitive KIEs were determined by reacting wt-RαO with 5:1 or 10:1 mixtures of perdeutero to perprotio fatty acids. Following acid quench and workup, the ratios of the aldehyde products at conversions from 1% to 5% were compared to the same ratio at 100% conversion. Measurements were performed by gas chromatography–mass spectrometry (GC–MS) on a Shimadzu GC17A/QP5050A equipped with a DB-5 ms column.

Noncompetitive KIEs were extracted from Michaelis–Menten plots obtained independently for the protio and deutero fatty acids. These experiments were performed at disparate enzyme concentrations that were varied by 10–50-fold to achieve similar rates for the labeled and unlabeled fatty acid substrates. Because perdeuterated and α,α-dideuterated fatty acids were used in this study, the observed $^Dk_{cat}$ and $^Dk_{cat}/K_M$(FA) consist of primary as well as secondary KIE contributions. The latter is expected to be $\leq$1.25 on the basis of precedents from related studies.[41,42]

Isotope Exchange. Isotope exchange experiments were conducted under an atmosphere of N_2, inside an MBraun glovebox, or in the presence of air. The incorporation of a single proton (from H_2O) into the α-position of the deuterium-labeled fatty acid was demonstrated under anaerobic conditions. A typical experiment involved preincubating protein solutions (1–10 μM) with 10 equiv of H_2O_2 and then stirring under N_2. The protein was added to a rigorously anaerobic solution of the deuterium-labeled fatty acid present at 100 μM. The reaction was quenched at time intervals between 0.5 and 8 h and the unreacted fatty acid isolated and analyzed. All samples were prepared for analysis by dichloromethane extraction of the acidified reaction mixture followed by dilution into a 50:50 methanol/0.1% ammonium acetate buffer. Control experiments, performed with solutions of deuterium-labeled fatty acids in the absence of protein, were treated identically to solutions containing either wt-RαO or the Tyr379Phe mutant. The fatty acid isotope composition was quantified by electrospray ionization mass spectrometry (ESI-MS) using a ThermoFinnigan LCQ Deca operating in negative ion mode.

Results

Enzyme Activation. Attempts have been made to observe formation of the oxidized prosthetic group upon treatment of
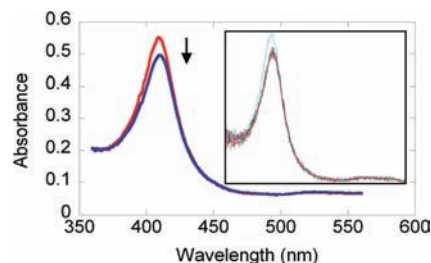
(39) The competitive KIE was calculated using the following equation, where [P-H]/[P-D] is the ratio of the integrated peak areas for the aldehyde products at ~1–5% conversion and [S_0-D]/[S_0-H] is the initial ratio of substrate isotopologues, which should be equivalent to the ratio of products at 100% conversion:

$$\frac{^Dk_{cat}}{K_M}(FA) = \frac{[P\text{-}H]}{[P\text{-}D]}\frac{[S_0\text{-}D]}{[S_0\text{-}H]}$$

A similar method is outlined in ref 40. By definition, the competitive KIE reflects the isotope effect on the second-order rate constant.

(40) Lewis, E. R.; Johansen, E.; Holman, T. R. *J. Am. Chem. Soc.* **1999**, *121*, 1395–1396.

(41) Grant, K. L.; Klinman, J. P. *Bioorg. Chem.* **1992**, *20*, 1–7.

(42) Rickert, K. W.; Klinman, J. P. *Biochemistry* **1999**, *37*, 12218–28.

Figure 1. UV–vis absorption spectra acquired by rapid-mixing, stopped-flow spectrophotometry upon reaction of RαO (4.5 μM) with 100 equiv of H_2O_2. The initial spectrum is shown in red and the final spectrum in blue. Spectra collected over the first 0.25 s are shown in the inset.
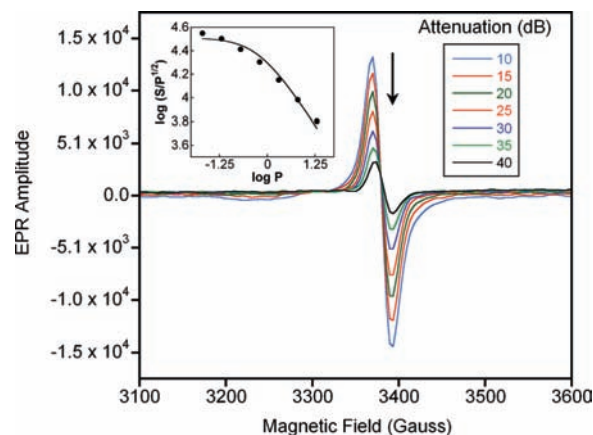

Figure 2. Power saturation of the EPR signal obtained upon reaction of wt-RαO (40 μM) with 10 equiv of H_2O_2. Data were collected at 15 K and analyzed as described in the Experimental Section. The inset shows the fitted data used to determine the power at half-saturation ($P_{1/2}$).

wt-Fe^{III}RαO with excess H_2O_2, in the absence of fatty acid, by monitoring the reaction using stopped-flow spectrophotometry. At concentrations of 1–5 μM wt-RαO, reactions with 50–500 equiv of H_2O_2 caused only slight spectral changes, as shown in Figure 1. An average H_2O_2 independent rate constant of 62 $\pm$ 12 s^{-1} was determined at 295 K. Optical changes on the millisecond time scale were indistinguishable from those acquired on longer time scales using conventional UV–vis spectrophotometry.[4b] The spectrum of the product is characterized by a slight bathochromic (red) shift and bleach of the Soret band. No evidence for Fe^{IV}=O(Por$^{•+}$) or Fe^{IV}=O(Por) was obtained; yet these species are readily observed when Tyr379Phe-RαO is treated with H_2O_2 under the same conditions.[4b]

EPR power saturation experiments corroborated the assignment of the persistent Tyr379$^{•}$.[4b] Solutions of wt-RαO and Tyr379Phe-RαO (40 μM) were prepared in air-saturated sodium phosphate buffer (pH 7.2, μ = 0.1 M) containing 25% glycerol and placed in sample tubes where they were manually mixed with 10 equiv of H_2O_2 at ambient temperature. Samples were frozen first at 193 K and then at 77 K. No EPR signal was discernible in the sample containing the Tyr379Phe mutant, whereas the expected signal at g = 2.0054 was observed in the sample containing wt protein.[37] Diminution of the signal amplitude associated with the Tyr379$^{•}$ in wt-RαO was observed at variable powers, under the conditions outlined in the Experimental Section, indicating $P_{1/2}$ = 0.6 mW at 15 K (Figure 2). Previous studies of heme proteins have shown this $P_{1/2}$ to

be characteristic of protein-derived radicals rather than the $Fe^{IV}=O(Por^{•+})$, which is also EPR-active.[43]

Upon oxidation of resting wt-RαO, Tyr379[•] is presumably formed concomitant with the reduction of $Fe^{IV}=O(Por^{•+})$ to $Fe^{IV}=O(Por)$. The absence of a detectable ferryl intermediate in the stopped-flow spectrophotometric experiments suggests that the latter process, along with the reduction of $Fe^{IV}=O(Por)$ back to $Fe^{III}(Por)$, occurs more rapidly than the initial oxidation of Fe^{III}-RαO by H_2O_2. These observations are consistent with Tyr oxidation rate constants as large as 460 ± 50 s^{-1} under similar conditions in COX-1.[44] Different behavior occurs in the structurally related heme peroxidases that do not use amino acid radicals for catalysis. In these cases, Tyr oxidation over distances comparable to those found in COX and RαO has been associated with rate constants of ≤ 5 s^{-1}.[45−47]

In light of its similarity to COX, it is surprising that RαO does not exhibit a significant peroxidase activity.[4b,24] Instead the enzyme exhibits a catalase-like activity that may protect it from overoxidation at high concentrations of H_2O_2.[48] Despite the lack of peroxidase activity in the presence of prototypical reducing agents,[49] the dioxygenase activity is affected upon exposure of RαO to H_2O_2, concomitant with an increase in the persistent EPR signal assigned to Tyr379[•]. Pretreatment with H_2O_2 has been observed to increase initial rates of O_2 consumption in a manner that depends on the preparation of protein and the identity of the fatty acid substrate. Such results are provided in the Supporting Information, where it is shown how the optimal concentration of H_2O_2 was determined for use in the steady-state kinetic experiments.

Steady-State Kinetics. Steady-state experiments employed 16:0, 12:0, and 10:0 to probe the effects of varying the O_2 and FA concentrations upon the apparent kinetic parameters. Because a large number of Michaelis−Menten plots were obtained in the course of these studies, only the salient results are presented below while the remainder are provided as Supporting Information.

A primary objective was to determine the kinetic mechanism of RαO. This analysis required evaluating the apparent rate constants $^{ap}k_{cat}$, $^{ap}k_{cat}/K_M(FA)$, and $^{ap}k_{cat}/K_M(O_2)$ in response to variable cosubstrate concentrations. Use of 12:0 and 10:0 facilitated these analyses by exposing the changes in apparent rate constants at low fatty acid and O_2 concentrations. Such measurements are more challenging with longer chain fatty acids, such as 16:0 and 9(Z),12(Z)-octadecadienoic acid (also
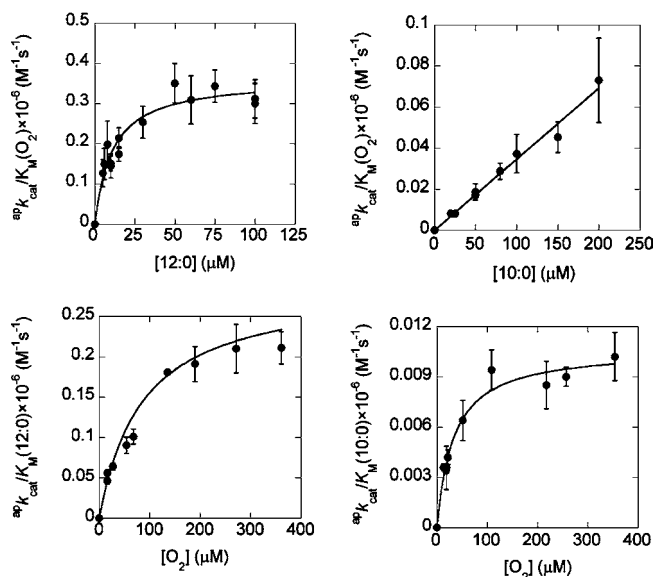

Figure 3. Apparent second-order rate constants for (protio) fatty acid oxidation in response to varying the concentration of the cosubstrate.

referred to as 18:2 or linoleic acid), because of the very low $K_M(FA)$ values which approach the detection limit of the O_2 electrode.

Another objective was to determine the limiting kinetic parameters so that the energetics of the Tyr379[•]-mediated H[•] abstraction step could be assessed. In the present study, experiments were most feasible with the native substrate, 16:0, because kinetic saturation readily occured. Comparisons to 12:0 were made possible by working at high O_2 and fatty acid concentrations.

Limiting values for k_{cat}, $k_{cat}/K_M(FA)$, and $k_{cat}/K_M(O_2)$ were obtained from the analysis of apparent kinetic parameters for all substrates except 10:0. In the latter case, $K_M(h_{19}\text{-}10:0)$ is estimated to be in excess of 750 μM, which is above the highest concentration that could reliably be used in the experiments, compromising the determination of k_{cat}. As depicted in Figure 3, the apparent second-order rate constants $^{ap}\{k_{cat}/K_M(h_{23}\text{-}12:0)\}$, $^{ap}\{k_{cat}/K_M(h_{19}\text{-}10:0)\}$ and the associated $^{ap}\{k_{cat}/K_M(O_2)\}$ increased upon raising the cosubstrate concentration.

Substrate Deuterium Kinetic Isotope Effects on $k_{cat}/K_M(FA)$. Substrate deuterium KIEs provide the critical information needed to test kinetic mechanisms and assess the degree of rate limitation by H[•] abstraction from the fatty acid C_α−H bond. Competitive and noncompetitive measurements were performed in this study to obtain the limiting KIEs $^Dk_{cat}$ and $^Dk_{cat}/K_M(FA)$, which are defined at concentrations $\geq 6K_M(O_2)$. The noncompetitive measurements employed disparate enzyme concentrations, whereas the competitive measurements were performed with the same enzyme concentration by analyzing solutions containing a mixture of the deuterium-labeled and unlabeled fatty acids. Therefore, the deuterium KIEs were confirmed to be independent of the RαO concentration over a wide range.

In Figure 4, typical Michaelis−Menten plots are shown for two protio and two deutero fatty acids that exhibit saturation kinetics. The $^Dk_{cat}$ values derived for 16:0 and 12:0 are 27 ± 3 and 102 ± 8, respectively. The former KIE is in good agreement with that previously reported (31 ± 5);[4b] however, the noncompetitively determined $^Dk_{cat}/K_M(16:0)$ is inaccurate due to the very small $K_M(d_{31}\text{-}16:0) \cong 2.4 \pm 1.2$ μM. As a result,

(43) (a) Yeh, H.-C.; Gerfen, G. J.; Wang, J.-S.; Tsai, A.-L.; Wang, L.-H. *Biochemistry* **2009**, *48*, 917−928. (b) Schunemann, V.; Lendzian, F.; Jung, C.; Contzen, J.; Barra, A.-L.; Sligar, S. G.; Trautwein, A. X. *J. Biol. Chem.* **2004**, *279*, 10919−30.

(44) Liu, J.; Seibold, S. A.; Rieke, C. J.; Song, I.; Cukier, R. I.; Smith, W. L. *J. Biol. Chem.* **2007**, *282*, 18233−18244. The temperature used for stopped-flow measurements was not specified and is therefore assumed to be ambient.

(45) Miller, V. P.; Goodin, D. B.; Friedman, A. E.; Hartmann, C.; Ortiz de Montellano, P. R. *J. Biol. Chem.* **1995**, *270*, 18413−18419.

(46) (a) Kimura, S.; Yamazaki, I. *Arch. Biochem. Biophys.* **1979**, *198*, 580−588. (b) Furtmüller, P. G.; Jantschko, W.; Regelsberger, G.; Jakopitsch, C.; Arnhold, J.; Obinger, C. *Biochemistry* **2002**, *41*, 11895. (c) Zederbauer, M.; Furtmueller, P. G.; Ganster, B.; Moguilevsky, N.; Obinger, C. *Biochem. Biophys. Res. Commun.* **2007**, *356*, 450−6.

(47) Yeh, H.-C.; Gerfen, G. J.; Wang, J.-S.; Tsai, A.-L.; Wang, L.-H. *Biochemistry* **2009**, *48*, 917−928.

(48) Zamocky, M.; Furtmueller, P. G.; Obinger, C. *Antioxid. Redox Signaling* **2008**, *10*, 1527−1548.

(49) No peroxidase activity was observed with the following reductants: phenol, 2-methoxyphenol, tetramethylphenylenediamine, or 2,2′-azinobis(3-ethylbenzothiazoline-6-sulfonic acid) (ABTS). For similar findings see ref 24a.
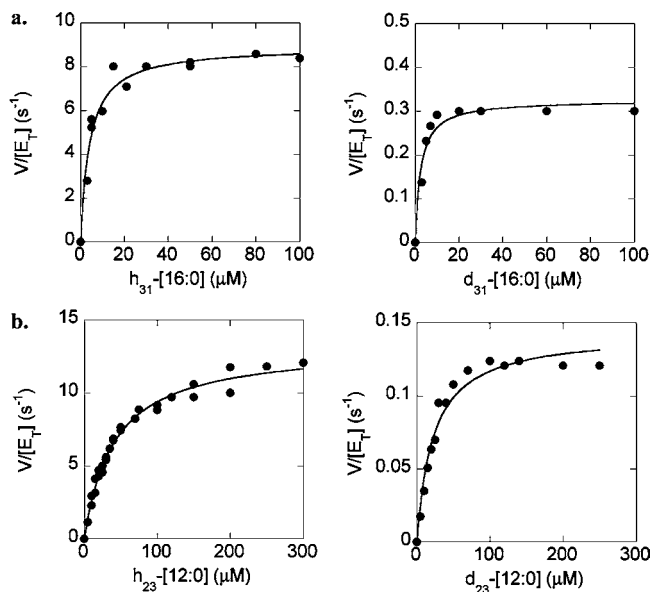
Figure 4. Michaelis–Menten plots used to determine noncompetitive deuterium KIEs upon the oxidation of 16:0 (a) and 12:0 (b) at saturating levels of O_2 (1.3 mM).
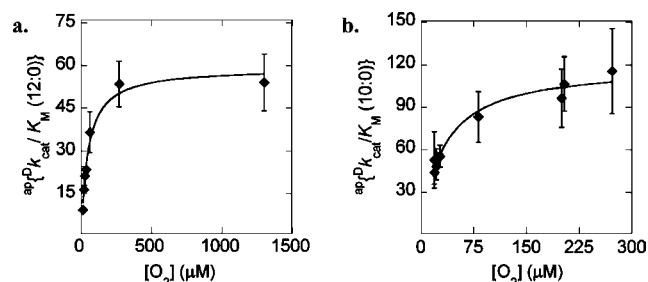

Figure 5. Variation of apparent deuterium KIEs with O_2 concentration. Measurements were performed competitively for 12:0 (a) and noncompetitively for 10:0 (b).

competitive KIE measurements were used to obtain a reliable estimate of $^D k_{cat}/K_M(16:0) = 33 \pm 4$. This KIE is within the error limits of the average $^D k_{cat} = 29 \pm 4$.

Competitive as well as noncompetitive measurements indicated $^D k_{cat}/K_M(12:0) = 59 \pm 5$ and 51 ± 8, respectively. The competitive KIE is considered more reliable than the noncompetitive KIE, which was determined at a single saturating O_2 concentration ($\sim$1.3 mM) versus extrapolation to O_2 saturation, as shown in Figure 5. As described in the Experimental section, the precision of the competitive KIE measurement derives from the resolution of GC–MS signals corresponding to the perprotio and perdeutero aldehyde products.[4b] Unfortunately, the precision is compromised for 10:0 due to significant overlap of the isotopic nonaldehyde products. Noncompetitive measurements at variable O_2 concentrations were, therefore, performed to obtain $^D k_{cat}/K_M(10:0) = 120 \pm 8$.

Evidence that the observed KIEs approach intrinsic values comes from the comparison of $^D k_{cat}$ to $^D k_{cat}/K_M(FA)$. Though it would be ideal to address this issue by comparing steady-state KIEs to pre-steady-state KIEs determined in the absence of O_2,[50] such measurements have not been undertaken due to the expected difficulty in directly observing changes in the Tyr379[•] concentration because of a potentially endothermic C_α–H

oxidation step (*vide infra*). In the case of the native substrate, similar values of $^D k_{cat}$ and $^D k_{cat}/K_M(16:0)$ suggest an intrinsic deuterium KIE of $\sim$30. Indistinguishable values of $^D k_{cat}$ and $^D k_{cat}/K_M(16:0)$ have also been observed at pH 10.0,[4b] where the deuterium KIEs (of $\sim$50) as well as the rate constants are elevated relative to those at pH 7.2.

In contrast to 16:0, the oxidation of 12:0 is characterized by kinetic complexity. The $^D k_{cat}$ of 102 is significantly larger than the $^D k_{cat}/K_M(12:0)$ of 59. This comparison suggests that substrate binding partially masks the KIE upon the second-order rate constant. A similar situation may obtain for 10:0; however, the inflated K_M for this fatty acid precludes the comparison of $^D k_{cat}/K_M(10:0)$ to $^D k_{cat}$. If fatty acid binding were partially rate limiting, $^D k_{cat}/K_M(10:0) = 120$ would actually represent a lower limit to the intrinsic KIE.

The limiting rate constants and deuterium KIEs extracted from Figures 3–5 are summarized in Table 1. The $k_{cat}/K_M(O_2)$ values were determined similarly, by extrapolation of $^{ap}\{k_{cat}/K_M(O_2)\}$ to saturating levels of each protio and deutero fatty acid. These data will be further analyzed in a forthcoming study.[30] Here it is simply noted that $k_{cat}/K_M(O_2)$ approximates 3×10^5 M^{-1} s^{-1} for h_{31}-16:0 and h_{23}-12:0 and that the rate constants are of the same order of magnitude for d_{31}-16:0 and d_{23}-12:0. The deuterium KIE upon $k_{cat}/K_M(O_2)$ is, therefore, much smaller than those observed upon k_{cat} and $k_{cat}/K_M(FA)$. Although $^D k_{cat}$ and $^D k_{cat}/K_M(FA)$ contain primary as well as secondary contributions, the values are well outside the semiclassical limits, even after correction for typical secondary deuterium KIEs.[41,42] Therefore, the competitive and noncompetitive deuterium KIEs determined to reflect rate-limiting C_α–H homolysis are clearly indicative of extensive hydrogen tunneling. Interestingly, this radical-mediated reaction in RαO gives rise to some of the largest deuterium KIEs that have been reported to date.[51]

Isotope Exchange Experiments. Tyr379[•]-containing RαO catalyzes isotope exchange of the pro-R hydrogen in the 2-position of the fatty acid with hydrogen from the solvent under anaerobic conditions.[52] Experiments were conducted by pretreating wt-RαO and Tyr379Phe-RαO with optimal concentrations of H_2O_2 followed by deoxygenation under N_2. The protein was then introduced into the deoxygenated solution of deuterium-labeled fatty acid. Control experiments were performed simultaneously using all components except for the protein. These solutions were stirred under N_2 at 298 K and samples collected for analysis at time intervals between 0.5 and 8 h. For comparison, experiments were also performed in air-saturated solutions, and the progress was monitored until 20–50% of the O_2 was consumed. All solutions were quenched and prepared for ESI-MS analysis following the procedure described in the Experimental Section.
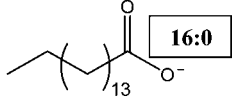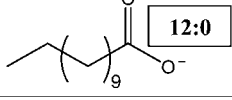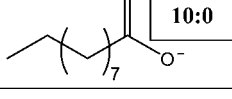
The results in Figure 6 clearly demonstrate that wt-RαO catalyzes exchange of the deuterium from the C_α–D bond with protons from the H_2O solvent in the absence of O_2. When O_2 is present, isotope exchange into the "unreacted" fatty acid is apparently inhibited; i.e., the deuterium does not wash out into the solvent. Importantly, no exchange occurs when the fatty acid is incubated with the Tyr379Phe mutant under identical conditions. These experiments provide compelling evidence that Tyr379[•] initiates fatty acid oxidation by H[•]/D[•] abstraction. The

(50) Cook, P. F.; Cleland, W. W. *Enzyme Kinetics and Mechanism*; Garland Science: New York, 2007.

(51) Klinman, J. P. *Chem. Phys. Lett.* **2009**, *471*, 179–193.

(52) Similar results were observed using D_2O and analyzing deuterium incorporation into the perprotio fatty acids.

Table 1. Rate Constants and Substrate Deuterium KIEs upon Fatty Acid C_α−H Oxidation[a]

Substrate	k_{cat} (s^{-1})	$^D k_{cat}$	$k_{cat}/K_M \times 10^{-6}$ (M^{-1}s^{-1})	$^D k_{cat}/K_M$ [b]
16:0 (13)	9.0 ± 1.0 [c]	29 ± 4 [c]	2.2 ± 0.4	33 ± 4 (c)
12:0 (9)	13.3 ± 0.9	102 ± 8	0.33 ± 0.01	59 ± 5 (c) 57 ± 8 (nc)
10:0 (7)	> 5.5 [d]	> 90 [e]	0.011 ± 0.001	120 ± 8 (nc)

[a] Values quoted are the average of at least two independent measurements. [b] Competitive (c) and noncompetitive (nc) KIEs were determined at O_2 saturation, i.e., $\geq 6K_M(O_2)$. [c] From ref 4b. [d] Lower limit from measurements at 750 μM h_{31}-10:0. [e] Estimated by varying O_2 at the limit of h_{19}- and d_{19}-10:0 solubility.
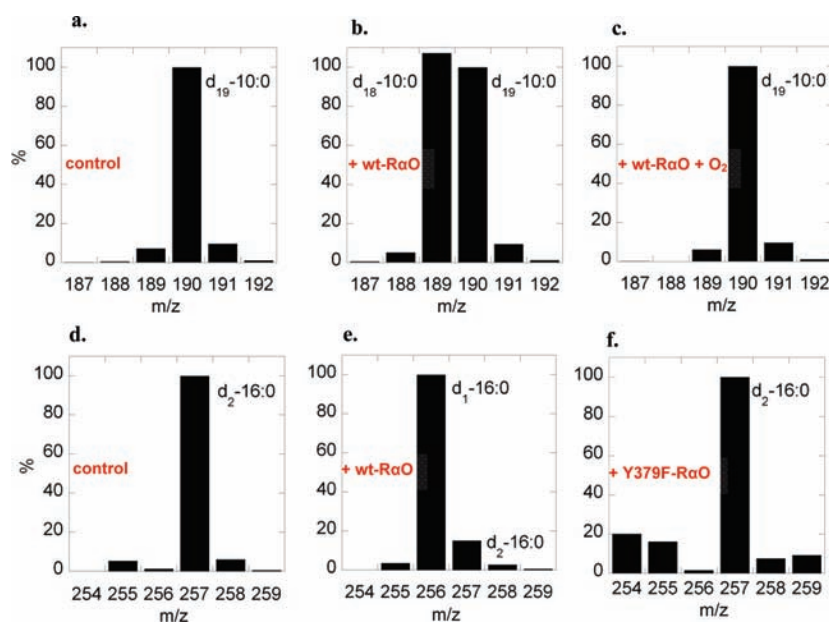

Figure 6. ESI-MS analysis of solvent isotope exchange into the unreacted fatty acid. All experiments were conducted with N_2-saturated solutions at 298 K unless noted: (a) d_{19}-10:0 in H_2O, (b) d_{19}-10:0 + wt-RαO in H_2O, (c) d_{19}-10:0 + wt RαO + O_2 (~258 μM) in H_2O (d) α,α-d_2-16:0 in H_2O, (e) α,α-d_2-16:0 + wt-RαO in H_2O, (f) α,α-d_2-16:0 + Tyr379Phe-RαO in H_2O.

inability of H_2O_2-activated Tyr379Phe-RαO to mediate hydrogen isotope exchange also argues convincingly against the involvement of $Fe^{IV}=O(Por^{•+})$ and $Fe^{IV}=O(Por)$ as well as other amino acid radicals that may be formed upon exposure of the heme proteins to H_2O_2.

As expected for stereospecific enzyme catalysis, only a single deuterium atom is lost to the solvent and a single protium is incorporated into the unreacted fatty acid. Thus, d_{18}-10:0 and α-d_1-16:0 are the only detectable products from solutions initially containing d_{19}-10:0 and α,α-d_2-16:0. That wt-RαO does not mediate loss of the deuterium label from fatty acids under aerobic conditions is attributed to slow exchange of H_2O with Tyr379-OD. Therefore, under normal catalytic conditions, the deuterium label is transferred from the fatty acid via Tyr379• into the 2(R)-hydroperoxide product. These results are consistent

with the absence of significant solvent KIEs on any of the steady-state kinetic parameters.[4b,30]

Discussion

Enzyme Activation. RαO undergoes 2e$^-$ oxidation by H_2O_2 at the $Fe^{III}(Por)$ prosthetic group to generate the Tyr379• cofactor. $Fe^{IV}=O(Por^{•+})$ is a likely intermediate; however, it does not accumulate to a detectable level under the experimental conditions. Therefore, it is uncertain whether $Fe^{IV}=O(Por^{•+})$ is the direct precursor to the Tyr379• intermediate, as observed in the homologous cyclooxygenases.[3] In RαO, reduction of $Fe^{IV}=O(Por)$ is also facile, resulting in $Fe^{III}(Por)$ as the only observable species on the millisecond to second time scale. The results are consistent with rapid ferryl formation in wt-RαO followed by amino acid oxidation at a rate much greater than that seen in the Tyr379Phe-RαO mutant.[4b] Stopped-flow spec-

trophotometry suggests Tyr379• formation with a H$_2$O$_2$-independent rate constant of $\geq$62 s^{-1} in the wt enzyme.

The proposed catalytic Tyr• is conserved in RαO and in COX, making comparisons of the two fatty acid oxidizing enzymes of interest. Whereas COX reacts with hydroperoxides to form multiple tyrosyl radicals and observable ferryl intermediates that are implicated in "suicide deactivation" of the enzyme,[6] RαO reacts with hydroperoxides in a controlled manner, generating a persistent Tyr• as the only observable intermediate during catalysis. Also in contrast to COX, RαO can turn over for several hours under ambient conditions, oxidizing all fatty acid present in solution.[4b,37] Regarding similarities of the two enzymes, COX exhibits a protective peroxidase activity that is independent of its dioxygenase activity,[3] while RαO catalyzes H$_2$O$_2$ disproportionation. That this reaction is independent of fatty acid oxidation is evidenced by the observation that wt-RαO and Tyr379Phe-RαO react with H$_2$O$_2$ at similar rates and efficiencies.

At this stage, it is unclear whether the absence of peroxidase activity in RαO is due to an intrinsic property of the enzyme or to its specificity for an exogenous reductant that has yet to be identified.[4a,24] The absence of peroxidase activity could reflect inaccessibility of reductants to the oxidized prosthetic group, which appears to be buried below the protein surface to a greater extent in RαO than in COX.[3,17] The structural issues notwithstanding, RαO's catalase-like activity[48] protects it from over-oxidation by excess H$_2$O$_2$ while allowing for enzyme activation.[37]

RαO is isolated with a trace amount of a spectroscopically observable radical resembling the catalytic species.[4b] An organic radical also appears in the structurally related fatty acid α-dioxygenase from *Arabidopsis thaliana*, but there the Tyr• has not been implicated in catalysis.[24] The presence of trace levels of Tyr379• in RαO could explain why addition of hydroperoxide initiators is not required for optimal dioxygenase activity.[4b] A significant rate enhancement is seen upon addition of H$_2$O$_2$ to 10:0 and 12:0 but not so much for 16:0. The difference is presumably due to accumulation of the 2(R)-hydroperoxide product, resulting in enzyme activation. The reaction is faster with the native substrate than with the shorter chain analogues, which exhibit lower apparent turnover rates due to their elevated K$_M$(FA).[37]

Fatty Acid Oxidation. Studies of RαO reveal a hyperbolic O$_2$-dependent increase in the apparent rate constants, $^{ap}k_{cat}$ and $^{ap}\{k_{cat}/K_M(FA)\}$, as well as in the apparent deuterium KIEs, $^{ap}\{^Dk_{cat}\}$ and $^{ap}\{^Dk_{cat}/K_M(FA)\}$, to limiting values for C$_\alpha$−H(D) homolysis. The latter results are indicative of reversible H• and D• tunneling at subsaturating O$_2$ concentrations and a transition to irreversible tunneling at saturating concentrations $\geq$6K$_M$(O$_2$).

The limiting k_{cat} values for protio fatty acids are relatively indistinguishable, varying from 9.0 (16:0) to 13.3 (12:0) to >5.5 (10:0) s^{-1}. The limiting $^Dk_{cat}$ values exhibit greater variation, increasing from 29 (16:0) to 102 (12:0) to >90 (10:0). The turnover rate constants for the deuterated fatty acids are more sensitive to varying the chain length. This effect is ostensibly a reflection of how the fatty acid is bound, relative to Tyr379•, in the active site. $^Dk_{cat}/K_M(FA)$ also increases with decreasing chain length, from 33 (16:0) to 58 (12:0) to 120 (10:0). Shortening the fatty acid chain also has a dramatic effect upon $k_{cat}/K_M(FA)$, decreasing from 2.2 × 10^6 (h_{31}-16:0) to 3.3 × 10^5 (h_{23}-12:0) to 1.1 × 10^4 (h_{19}-10:0) M^{-1} s^{-1} and from 6.7 × 10^4 (d_{31}-16:0) to 5.7 × 10^3 (d_{23}-12:0) to 9.2 × 10^1 (d_{19}-10:0) M^{-1} s^{-1}. In addition to the interaction between fatty acid carboxylate and His311,

noncovalent interactions within the enzyme−substrate (Michaelis) complex could assist in positioning the fatty acid so that the reactive C$_\alpha$−H(D) approaches the Tyr379•. The weaker fatty acid binding affinity, which is at least partially manifest in the increasing K$_M$(FA), should impact the distance over which the hydrogen must transfer. Increasing this distance is expected to result in diminution of the rate constant and an inflation of the deuterium KIE.

Given the degree of rate limitation by C$_\alpha$−H(D) homolysis, comparisons of $^Dk_{cat}$ to $^Dk_{cat}/K_M(FA)$ can be used to infer intrinsic KIEs.[53] That $^Dk_{cat}$ = 29 ± 4 is indistinguishable from $^Dk_{cat}/K_M(16:0)$ = 33 ± 4 indicates that the intrinsic KIE is fully expressed at pH 7.2. A similar relationship has been reported at pH 10.0, where $^Dk_{cat}$ = 54 ± 7 and $^Dk_{cat}/K_M(16:0)$ =53 ± 5.[4b] In view of the results from the present study, the increased intrinsic KIE for 16:0 under basic conditions is attributed to a change in positioning of the bound fatty acid in the active site. Partial rate limitation by fatty acid binding is indicated for the medium chain length fatty acid, where $^Dk_{cat}$ = 102 ± 8 differs significantly from $^Dk_{cat}/K_M(12:0)$ = 59 ± 5. Although $^Dk_{cat}$ cannot be determined for the shortest chain substrate because of its elevated K$_M$(10:0), a value of >90 is estimated from the apparent turnover rate constants at the limit of fatty acid solubility. Despite the inability to observe saturation kinetics, the results suggest a large degree of rate limitation by C$_\alpha$−H(D) bond cleavage. If this contribution to the second-order rate constant were partially masked by fatty acid binding, $^Dk_{cat}/K_M(10:0)$ = 120 would actually represent a lower limit to the intrinsic KIE.

The closeness of $^Dk_{cat}$ and $^Dk_{cat}/K_M(FA)$ to the intrinsic KIEs indicates that K$_M$(FA) should be similar for the protio and deutero fatty acids. Furthermore, K$_M$(FA) should be comparable to K$_d$, the dissociation constant for the enzyme−fatty acid complex.[53] Assuming a simple two-step mechanism, where the fatty acid binds reversibly prior to C$_\alpha$−H homolysis, K$_d$ is estimated to range from 4 μM (16:0) to $\sim$40 μM (12:0) to $\geq$750 μM (10:0). These estimates correspond to free energies of −7.3 kcal mol^{-1} (16:0), −5.9 kcal mol^{-1} (12:0), and $\leq$−4.2 kcal mol^{-1} (10:0), which reflect stabilization of the Michaelis complex with respect to the free oxidized enzyme and fatty acid.

To briefly summarize, the hydrogen transfer distance is expected to be a primary determinant of the deuterium KIE. This conclusion is supported by the observed trends which result in the largest deuterium KIE being observed for the least tightly bound fatty acid. Elongating this distance in the Michaelis complexes is expected to diminish the probability of protium tunneling to a lesser extent than the probability of deuterium tunneling. There is also likely to be a significant increase in thermal activation energy required to achieve the configuration of heavy nuclei conducive to deuterium tunneling, as observed in numerous studies where semiclassical descriptions of hydrogen transfer are insufficient.[51]

A modified version of quantum mechanical Marcus Theory[54] has been implemented to explain a wide range of large and small deuterium KIEs on proton-coupled electron transfer/hydrogen atom transfer reactions. These nonadiabatic formalisms separate the electronic coupling and Franck−Condon overlap associated

(53) Klinman, J. P.; Matthews, R. G. *J. Am. Chem. Soc.* **1985**, *107*, 1058–60.

(54) (a) Marcus, R. A.; Sutin, N. *Biochim. Biophys. Acta* **1985**, *811*, 265–322. (b) Kamerlin, S, C. L.; Warshel, A. *Proteins: Structure, Function, Bioinf.* **2010**, *78*, 1339–1375. (c) Hammes-Schiffer, S. *Acc. Chem. Res.* **2006**, *39*, 93–100.

Scheme 1. Proposed Mechanism of Anaerobic Isotope Exchange Mediated by RαO
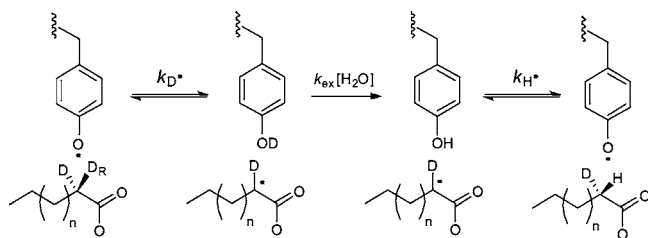
with the hydrogen isotopes' nuclear wave functions from the free energy barrier $\Delta G^{\ddagger}$. In the future, it will be interesting to determine whether such treatments can reproduce the rate constants and very large deuterium KIEs reported here for Tyr$^{\bullet}$-mediated $C_{\alpha}-H$ homolysis in RαO.

Effect of Molecular Oxygen. Studies of the mechanism by which RαO reacts with molecular oxygen are due to appear in a forthcoming paper.[30] The results presented here are discussed within the context of the kinetic mechanism. The data in Figure 3 reveal a dependence of $^{ap}\{k_{cat}/K_M(O_2)\}$ upon the fatty acid concentration as well as a dependence of $^{ap}\{k_{cat}/K_M(FA)\}$ upon the O_2 concentration in the reactions of 12:0 and 10:0. Such results frequently point to sequential kinetic mechanisms;[23,50] however, these mechanisms can be excluded for RαO because of the results in Figure 5, which reveal increases in the apparent deuterium KIEs, $^{ap}\{^{D}k_{cat}/K_M(FA)\}$ and $^{ap}\{^{D}k_{cat}\}$, upon raising the concentration of O_2.[55]

Additional mechanistic insight is derived from the limiting kinetic parameters associated with the oxidation of the protio and deutero fatty acids. $k_{cat}/K_M(O_2)$, determined for both 12:0 and 16:0 isotopologues, is on the order of 10^5 M^{-1} s^{-1}. Thus, $^{D}k_{cat}/K_M(O_2)$ is quite small compared to the very large $^{D}k_{cat}$ and $^{D}k_{cat}/K_M(FA)$. These results, together with the trends in apparent second-order rate constants with increasing cosubstrate concentration, are consistent with a mechanism involving $C_{\alpha}-H$ cleavage prior to O_2 trapping of the α-carbon radical. At concentrations in the physiological range, i.e., ~50 μM O_2, the rate-limiting step occurs *after* O_2 enters the catalytic cycle. On the basis of the magnitude of $k_{cat}/K_M(O_2)$, this step most likely involves an activation-controlled rather than diffusion-controlled process, such as reduction of the putative 2(R)-peroxyl radical. A detailed analysis of this mechanism, employing competitively determined oxygen-18 KIEs and DFT calculations performed on structures of potential transition states and intermediates, is the subject of a forthcoming paper.[30]

The reversibility of the initial hydrogen transfer during RαO catalysis is further evidenced by isotope exchange experiments under anaerobic conditions, revealing that wt-RαO catalyzes replacement of a single deuterium from α,α-d_2-16:0 and d_{19}-10:0 by protium from the H_2O solvent. Isotope exchange into the unreacted fatty acid is surprisingly sensitive to the presence of O_2. Inhibition of exchange, observed when O_2 is present, suggests a slow rate of solvent isotope incorporation into the active site Tyr379. Apparently, O_2 trapping of the fatty acid-derived radical and reduction of the putative 2(R)-peroxyl radical intermediate out-compete the Tyr O$-$D exchange with H_2O illustrated in Scheme 1.

That solvent isotope exchange lags behind fatty acid α-dioxygenation in RαO resembles the behavior proposed

in other enzymes, such as galactose oxidase[56] and possibly soybean lipoxygenase,[57] where retention of hydrogen from the substrate gives rise to a significant deuterium KIE upon $k_{cat}/K_M(O_2)$. In the latter case, the reported $^{D}k_{cat}/K_M(O_2)$ of ~4 may fall within the limits of error. Measurements of this type are complicated by artifacts encountered when $K_M(O_2)$ for the deuterated substrate is greatly suppressed to offset a very large deuterium KIE upon k_{cat}. The proposal that the deuterium label from the fatty acid is retained at Tyr379 in RαO, due to slow solvent isotope exchange with active site residues, is consistent with the absence of solvent KIEs or a discernible change in $^{D}k_{cat}$ or $^{D}k_{cat}/K_M(FA)$ when experiments are conducted in D_2O instead of H_2O.

Analysis of the Kinetic Mechanism. The cumulative results obtained in this study are consistent with the minimal mechanism depicted in Scheme 2, where E_{ox} and E_{red} reflect the redox state of Tyr379. The FA, FAO$_2^{\bullet}$, and P correspond to the fatty acid substrate, 2(R)-peroxyl radical, and the 2-(R)(hydro)peroxide product. A prime symbol is used to indicate that the protonation state of the products formed in the first irreversible step is unclear. In this description, cleavage of the fatty acid $C_{\alpha}-H$ bond occurs reversibly prior to reversible O_2 radical trapping and rate-limiting reduction of the 2(R)-peroxyl radical to eventually form the 2(R)-hydroperoxide product. The scheme accounts for the observation that $C_{\alpha}-H$ homolysis (k_3) is reversible at low concentrations of O_2 and that reduction of the 2(R)-peroxyl radical intermediate (k_7) becomes the first irreversible step.

The mechanism corresponding to steps after O_2 enters the catalytic cycle is the subject of a separate study.[30] In the present context, retention of the hydrogen from the fatty acid within the active site is expected to result in a small deuterium KIE upon $k_{cat}/K_M(O_2)$. Only an upper limit has been estimated because $K_M(O_2)$ for the deuterated substrate is close to the limit of detection. Importantly, kinetic expressions derived for the mechanism in Scheme 2 can be used to predict the hyperbolic dependence of the apparent $k_{cat}/K_M(O_2)$ and $k_{cat}/K_M(FA)$ on the cosubstrate concentrations, together with the O_2 depedence of the apparent $^{D}k_{cat}/K_M(FA)$. Explicit consideration of a small KIE on k_7 should have little effect.

The kinetic mechanism resembles one considered by Glickman and Klinman in studies of soybean lipoxygenase (LOX),[57] which oxidizes linoleic acid using an Fe$^{III}-$OH cofactor.[58] The oxidation of a weak bisallylic C$-$H bond was proposed to be irreversible on the basis of the very large $^{D}k_{cat}$ of ~80. Subsequent trapping of the delocalized fatty acid radical by O_2 was proposed to be the first irreversible step and thus the origin of regio- and stereo-specificity.[59] The situation is different in RαO, where reactions of the fatty acid and O_2 are linked by a reversible $C_{\alpha}-H$ homolysis step.

Kinetic equations were derived for the observed deuterium KIEs in RαO following Cleland's method of net rate constants.[60] For the purposes of this analysis, k_3 and k_4 were considered to be the only hydrogen isotope sensitive steps in Scheme 2. Although there is likely to be a small KIE upon

(55) Miller, S. M.; Klinman, J. P. *Methods Enzymol.* **1982**, *87*, 711–32.
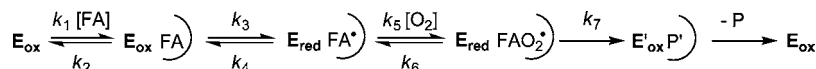
(56) Humphreys, K. J.; Mirica, L. M.; Wang, Y.; Klinman, J. P. *J. Am. Chem. Soc.* **2009**, *131*, 4657–4663.

(57) Glickman, M. H.; Klinman, J. P. *Biochemistry* **1996**, *35*, 12882–12892.

(58) Scarrow, R. C.; Trimitsis, M. G.; Buck, C. P.; Grove, G. N.; Cowling, R. A.; Nelson, M. J. *Biochemistry* **1994**, *33*, 15023–35.

(59) Knapp, M. J.; Klinman, J. P. *Biochemistry* **2003**, *42*, 11466–11475.

(60) (a) Cook, P. F.; Yoon, M. Y.; Hara, S.; McClure, G. D., Jr. *Biochemistry* **1993**, *32*, 1795. (b) Cleland, W. W. *Kinet. Biochem.* **1975**, *14*, 3220–4.

Scheme 2. Proposed Minimal Mechanism of Fatty Acid Oxidation by RαO

$$E_{ox} \underset{k_2}{\overset{k_1\,[FA]}{\rightleftharpoons}} E_{ox}\;FA) \underset{k_4}{\overset{k_3}{\rightleftharpoons}} E_{red}\;FA^\bullet) \underset{k_6}{\overset{k_5\,[O_2]}{\rightleftharpoons}} E_{red}\;FAO_2^\bullet) \overset{k_7}{\longrightarrow} E'_{ox}\,P') \overset{-\,P}{\longrightarrow} E_{ox}$$

k_7 detectable under certain conditions,[30] its neglect has little impact upon the following analysis, which concentrates upon the steps before O_2 enters the catalytic cycle. The apparent deuterium KIE on $k_{cat}/K_M(FA)$ is expressed according to eq 3. Terms include the intrinsic deuterium KIE and equilibrium isotope effect on C_α–H homolysis, $^Dk_3$ and $^D(k_3/k_4)$, respectively, as well as the forward and reverse commitment factors, $C_f = k_3/k_2$ and $C_r = k_4/k_5[O_2]\,(1 + k_6/k_7)$. It is further noted that the influence of k_7 is limited to the C_r term and that it is moderated by the magnitude of k_6.

$$^{ap}\left\{\frac{^Dk_{cat}}{K_M}(FA)\right\} = \frac{^Dk_3 + C_f + {}^D\!\left(\dfrac{k_3}{k_4}\right)C_r}{1 + C_f + C_r} \tag{3}$$

The term $^D(k_3/k_4)$, representing the equilibrium isotope effect on H$^\bullet$ transfer from the fatty acid C_α–H bond to Tyr379$^\bullet$, was calculated from the relevant stretching frequencies obtained using the DFT method described in the Experimental Section. Energy-minimized structures of 4-hydroxyphenylacetate and butanoate were used as models for Tyr379 and the longer chain fatty acids. The equilibrium isotope effect derives from the zero-point energy differences calculated from the normal mode stretching frequencies: ν(O–H) = 3528.6 cm^{-1}, ν(O–D) = 2568.4 cm^{-1}, ν(C$_\alpha$–H) = 3008.5 cm^{-1}, and ν(C$_\alpha$–D) = 2189.9 cm^{-1}. The difference in zero-point energy is found to be 70.8 cm^{-1}. Neglecting entropic contributions, this energy difference can be equated to $\Delta\Delta G^\circ = 0.202$ kcal mol^{-1}, which corresponds to $^D(k_3/k_4) = 1.4$ at 295 K.

The following analyses are intended to address how the proposed mechanism in Scheme 2 accommodates reversible C_α–H cleavage in light of the steady-state KIE expressions. First, it is noted that, in solution, O_2 trapping of carbon radicals typically occurs with rate constants that approach the diffusion limit, i.e., with values on the order of 10^9 M^{-1} s^{-1}.[61] A smaller rate constant, on the order of 10^7 M^{-1} s^{-1}, has been proposed for linoleic acid oxidation in soybean lipoxygenase and attributed to irreversible O_2 trapping of the delocalized pentadienyl radical; however, reversible O_2 trapping followed by rate-limiting peroxyl radical reduction could not be excluded.[59] Rate constants for O_2 dissociation from related peroxyl radicals, corresponding to k_6 in Scheme 2, have been examined and correlated to C–O bond dissociation energies.[62] k_6 is expected to be $\sim$10^3 s^{-1} for the stable conjugated peroxyl radicals produced by lipoxygenase, whereas k_6 values of $\sim$10^6 s^{-1} are characteristic of nonconjugated peroxyl radicals with weaker C–O bonds, resembling the 2(R)-peroxyl radical intermediate formed in RαO.

In light of results from the literature,[61,62] the 2(R)-peroxyl radical intermediate in RαO is considered to form with k_5 on the order of 10^9 M^{-1} s^{-1} and undergo O_2 dissociation with k_6 on the order of 10^6 s^{-1}. These estimates suggest a favorable equilibrium constant of 10^3 M^{-1} for 2(R)-peroxyl radical formation. Assuming a simple two-step process, involving initial

combination of the α-carbon radical with O_2, the observed $k_{cat}/K_M(O_2)$ of $\sim$10^5 M^{-1} s^{-1} divided by the O_2 association constant (K_a = 10^3 M^{-1}) gives k_7 = 10^2 s^{-1} for rate-limiting 2(R)-peroxyl radical reduction. In comparison, rate constants of $\sim$10^6 M^{-1} s^{-1} have been reported for bimolecular H$^\bullet$ transfer from α-tocopherol to lipid-derived peroxyl radicals.[62b]

Considering the above-mentioned rate constants, the contribution of k_6/k_7 to the reverse commitment factor is on the order of 10^4, such that $C_r = k_4/k_5[O_2](1 + 10^4)$. Thus, a small KIE on k_7 would have little effect upon C_r. That the apparent $^Dk_{cat}/K_M(FA)$ approaches a limiting value independent of the O_2 concentration (as shown in Figure 5) is consistent with C_r approaching 0 as the O_2 concentration is raised to saturating levels. The result is consistent with an expression for the limiting $^Dk_{cat}/K_M(FA)$ given by eq 4. Here $^Dk_3$ is moderated only by the forward commitment to catalysis. Because k_3 is the only term $^Dk_{cat}/K_M(FA)$ has in common with $^Dk_{cat}$, defined by eq 5, the comparison of KIEs can reveal the extent to which C_α–H cleavage is the first irreversible/rate-limiting step.

$$\frac{^Dk_{cat}}{K_M}(FA) = \frac{^Dk_3 + \dfrac{k_3}{k_2}}{1 + \dfrac{k_3}{k_2}} \tag{4}$$

$$^Dk_{cat} = \frac{^Dk_3 + \dfrac{k_3}{k_7}}{1 + \dfrac{k_3}{k_7}} \tag{5}$$

The following analysis was performed to test how the expressions derived from the mechanism in Scheme 2 quantitatively reproduce the KIEs upon 12:0 and 10:0 oxidation upon lowering the O_2 concentration. The transition from reversible to irreversible C_α–H homolysis upon raising the concentration of O_2, suggests that H$^\bullet$ abstraction by Tyr379$^\bullet$ ranges from slightly endothermic to thermoneutral. Assuming $\Delta G^\circ = 0$ kcal mol^{-1} for this step in Scheme 2 and taking the average k_{cat} for the protio fatty acids to be k_3 = 10 s^{-1}, k_4 is constrained to be 10 s^{-1}.

First, the oxidation of 12:0 is considered under the premise that $^Dk_{cat}$ = 102 is equivalent to the intrinsic deuterium KIE on the initial hydrogen atom transfer step, $^Dk_3$. This calculation employs eq 3 along with the computed $^D(k_3/k_4)$ = 1.4, C_f = 0.76 from eq 4, and C_r = (10^{-4} M^{-1})/[O_2] derived from k_4 = 10 s^{-1}, k_5 = 10^9 M^{-1} s^{-1}, k_6 = 10^6 s^{-1}, and k_7 = 10^2 s^{-1}. As observed in Figure 5a, the limiting $^Dk_{cat}/K_M(12{:}0)$ is predicted to drop from its observed maximum of 59 to an $^{ap}\{^Dk_{cat}/K_M(12{:}0)\}$ of 16 at 20 μM O_2.

The apparent KIE for 10:0 oxidation at subsaturating O_2 concentrations can also be modeled under the assumption that the measured $^Dk_{cat}/K_M(10{:}0)$ = 120 is equivalent to $^Dk_3$. Using this value, together with $^D(k_3/k_4)$ = 1.4, C_f = 0, and a somewhat smaller C_r = (3.0 × 10^{-5} M^{-1})/[O_2] in eq 3, predicts a drop from the maximum of 120 to an $^{ap}\{^Dk_{cat}/K_M(10{:}0)\}$ of 45 at 20 μM O_2. The experimental results in Figure 5b are reproduced, thus validating the proposed mechanism and the derived kinetic expressions.

(61) Maillard, B.; Ingold, K. U.; Scaiano, J. C. *J. Am. Chem. Soc.* **1983**, *105*, 5095–5099.
(62) (a) Tallman, K. A.; Roschek, B., Jr.; Porter, N. A. *J. Am. Chem. Soc.* **2004**, *126*, 9240–9247. (b) Pratt, D. A.; Mills, J. H.; Porter, N. A. *J. Am. Chem. Soc.* **2003**, *125*, 5801–5810.

Scheme 3. Proposed Tyr•-Mediated Fatty Acid α-Dioxygenase Mechanism
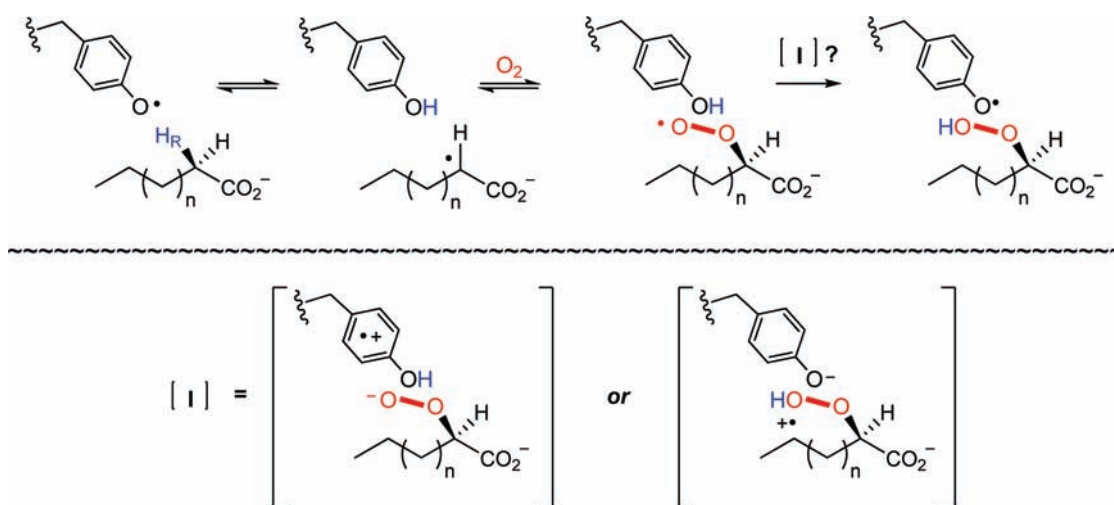
Thermodynamics of Tyr•-Mediated C_α−H Homolysis. The present studies reveal that Fe^{III}-wt-RαO is activated by H_2O_2.[37] The form of the enzyme resulting from this reaction contains a persistent Tyr379• and enhanced fatty acid dioxygenase activity.[4b] In contrast, the Tyr379Phe mutant does not exhibit such reactivity. Treatment with H_2O_2 merely oxidizes the prosthetic group to the Fe^{IV}=O(Por•+) state, which decays to Fe^{IV}=O(Por) and back to Fe^{III}(Por) using two reducing equivalents of unknown origin.

Despite the accessibility of the high oxidizing Fe^{IV}=O(Por•+) and Fe^{IV}=O(Por) in wt-RαO and in the Tyr379Phe mutant, these intermediates do not mediate fatty acid C_α−H oxidation. Instead a protein-derived radical initiates this transformation. Structural factors facilitate binding of the fatty acid in proximity to the persistent Tyr379•, a radical that is stabilized relative to the ferryl prosthetic group yet still maintains the thermodynamic ability to abstract a hydrogen atom from the α-position of various fatty acids. Typical C_α−H bond dissociation energies are between 90 and 94 kcal mol^{-1},[63] whereas phenolic bond dissociation energies span a larger range, from 80 to 90 kcal mol^{-1}, depending on the environment.[64,65] On these grounds, the initial H• transfer step in RαO is expected to be somewhat endothermic or close to thermoneutral, consistent with the kinetic analyses described above.

Scheme 3 depicts the detailed chemical mechanism proposed for RαO in which reversible H• abstraction is kinetically driven by reduction of O_2 to the fatty acid 2(R)-hydroperoxide product. As mentioned above, $k_{cat}/K_M(O_2)$ of ~10^5 M^{-1} s^{-1} reflects steps beginning with combination of O_2 and the fatty acid derived radical up to 2(R)-peroxyl radical reduction. The small magnitude of the observed rate constant is ostensibly more consistent with an activation-controlled process than a diffusion-controlled process, such as O_2 trapping of a radical or product release. Presently, it is unclear whether the 2(R)-hydroperoxide product is formed concomitant with regeneration of the catalytic Tyr•. Mechanisms of concerted or sequential proton-coupled electron transfer (PCET) are possible, as depicted in Scheme 3.

Concerted PCET is thermodynamically favored over the sequential mechanism where a high-energy intermediate is necessarily formed, as depicted in brackets in the scheme. In this study, hydrogen atom transfer is seen as a specific type of concerted proton-coupled electron transfer occurring with approximately the same $\Delta G°$. Like the initiating C_α−H homolysis, reoxidation of Tyr379 by the 2(R)-peroxyl radical is expected to be close to thermoneutral on the basis of the fatty acid hydroperoxide (OO−H) bond dissociation energies of 85−90 kcal mol^{-1} [66−68] and tyrosine (O−H) bond dissociation energies in the same range.[64,65] In general, bimolecular rate constants on the order of 10^6 M^{-1} s^{-1} are seen for concerted PCET/hydrogen atom transfer reactions of hydroxylic species and oxyl radicals in the solution phase.[68] k_7 of ~10^2 s^{-1}, corresponding to the first irreversible step in Schemes 2 and 3, suggests that the thermodynamic barrier can be as high as 14.5 kcal mol^{-1} as expected for a sequential PCET, where either electron or proton transfer is partially rate-limiting.

Conclusions

The kinetic mechanism of rice α-(di)oxygenase has been examined with C_{10}, C_{12}, and C_{16} saturated fatty acids. Catalysis is most likely initiated by H• abstraction from the fatty acid by Tyr379•. The reversibility of this step is established by the dependence of apparent second-order rate constants and attendant deuterium KIEs upon the O_2 concentration as well as solvent isotope exchange experiments that reveal inhibition by O_2. The observation that isotope exchange is mediated by wt-RαO but not the Tyr379Phe mutant reinforces the proposal that Tyr379• is the initiator of catalytic fatty acid α-dioxygenation.

Another intriguing finding concerns the dependence of deuterium KIEs upon the fatty acid chain length. Shortening the carbon chain from 16:0 to 10:0 reduces the fatty acid binding

(63) (a) Wenthold, P. G.; Squires, R. R. *J. Am. Chem. Soc.* **1994**, *116*, 11890–7. (b) Rauk, A.; Yu, D.; Taylor, J.; Shustov, G. V.; Block, D. A.; Armstrong, D. A. *Biochemistry* **1999**, *37*, 9089–9096.

(64) (a) Jovanovic, S. V.; Harriman, A.; Simic, M. G. *J. Phys. Chem.* **1986**, *90*, 1935–9. (b) Harriman, A. *J. Phys. Chem.* **1987**, *91*, 6102–4.

(65) (a) Mulder, P.; Korth, H.-G.; Pratt, D. A.; DiLabio, G. A.; Valgimigli, L.; Pedulli, G. F.; Ingold, K. U. *J. Phys. Chem. A* **2005**, *109*, 2647–2655. (b) Nara, S. J.; Valgimigli, L.; Pedulli, G. F.; Pratt, D. A. *J. Am. Chem. Soc.* **2010**, *132*, 863–872. (c) Blomberg, M. R. A.; Siegbahn, P. E. M.; Styring, S.; Babcock, G. T.; Aakermark, B.; Korall, P. *J. Am. Chem. Soc.* **1997**, *119*, 8285–8292.

(66) Blanksby, S. J.; Ramond, T. M.; Davico, G. E.; Nimlos, M. R.; Kato, S.; Bierbaum, V. M.; Lineberger, W. C.; Ellison, G. B.; Okumura, M. *J. Am. Chem. Soc.* **2001**, *123*, 9585–9596.

(67) Das, T. N.; Dhanasekaran, T.; Alfassi, Z. B.; Neta, P. *J. Phys. Chem. A* **1998**, *102*, 280–284.

(68) Huang, M. L.; Rauk, A. *J. Phys. Org. Chem.* **2004**, *17*, 777–786.

affinity and, most likely, accounts for the decrease in k_{cat}/K_M(FA) by 2 orders of magnitude. Elongation of the hydrogen tunneling distance may be inferred from the escalating deuterium KIEs associated with the less tightly bound substrates. Despite differences in the fatty acid chain length, k_{cat} corresponding to C_α−H homolysis is relatively invariant with values of 9.0 ± 1.0 (h_{31}-16:0), 13.3 ± 0.9 (h_{23}-12:0) and >5.5 (h_{19}-10:0) s^{-1}. Somewhat larger variations in k_{cat} are indicated for C_α−D homolysis, where values range from 0.31 ± 0.04 (d_{31}-16:0) to 0.13 ± 0.01 (d_{23}-12:0) to >0.06 (d_{19}-10:0) s^{-1}. The results suggest an increase in $^Dk_{cat}$ as the fatty acid chain length and binding affinity decrease. The origins of these effects remain to be more thoroughly tested through studies of the temperature-dependent intrinsic deuterium kinetic isotope effects.

A dependence of $^Dk_{cat}$ upon the fatty acid chain length may be expected on the basis of intrinsic barriers, where that accompanying C−D homolysis is greater than that accompanying C−H homolysis.[51] Such barriers can be determined from studies of primary kinetic isotope effects as a function of temperature[69] and from studies of isotopic rate constants as a function of $\Delta G°$.[70] Within the terminology of Marcus Theory,[54a] the reorganization energy required to attain the activated configuration (or transition state) conducive to hydrogen tunneling may be greater for deuterium than for protium. This effect, which is similar to thermally activated "gating" or "distance sampling",[51,69] derives from the shorter distance required for deuterium transfer because of its heavier mass and poorer wave function overlap in the ground vibrational state than that associated with protium.[69b]

In conclusion, rice α-(di)oxygenase presents an ideal model system for investigating a growing class of heme and tyrosyl radical-containing enzymes. The present studies have allowed detailed mechanistic insights involving the observation of reversible hydrogen atom tunneling upon oxidation of a relatively robust C−H bond by a persistent tyrosyl radical. New questions have emerged concerning how to explain the very large deuterium kinetic isotope effects on such reactions and their apparent correlation to substrate binding affinity. It will be interesting to determine whether the nonadiabatic formalisms established to treat concerted proton-coupled electron transfer[69b] can be used to model the tyrosyl radical-mediated reactions uncovered in this study.

Supporting Information Available: Additional kinetic and spectroscopic characterization. This material is available free of charge via the Internet at http://pubs.acs.org.

JA104180V

(69) (a) Knapp, M. J.; Rickert, K.; Klinman, J. P. *J. Am. Chem. Soc.* **2002**, *124*, 3765–3774. (b) Hatcher, E.; Soudackov, A. V.; Hammes-Schiffer, S. *J. Am. Chem. Soc.* **2004**, *126*, 5763–5775.
(70) Brinkley, D. W.; Roth, J. P. *J. Am. Chem. Soc.* **2005**, *127*, 15720–1572.